



Research Article http://pubs.acs.org/journal/acscii

Emergence of Ferrichelatase Activity in a Siderophore-Binding Protein Supports an Iron Shuttle in Bacteria

Nathaniel P. Endicott, Gerry Sann M. Rivera, Jinping Yang, and Timothy A. Wencewicz*



Cite This: ACS Cent. Sci. 2020, 6, 493-506



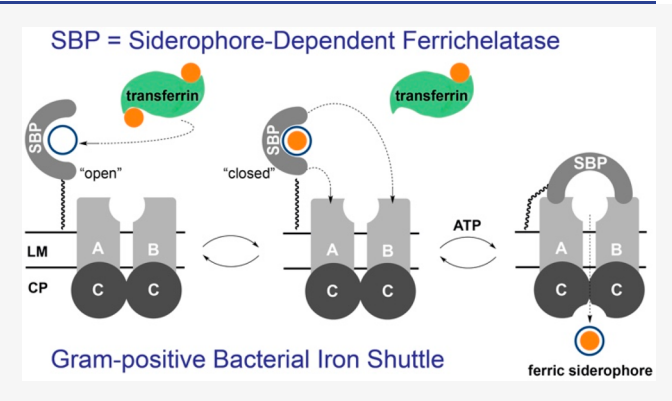
ACCESS I

III Metrics & More

Article Recommendations

Supporting Information

ABSTRACT: Siderophores are small-molecule high-affinity multidentate chelators selective for ferric iron that are produced by pathogenic microbes to aid in nutrient sequestration and enhance virulence. In Gram-positive bacteria, the currently accepted paradigm in siderophore-mediated iron acquisition is that effluxed metal-free siderophores extract ferric iron from biological sources and the resulting ferric siderophore complex undergoes diffusioncontrolled association with a surface-displayed siderophore-binding protein (SBP) followed by ABC permease-mediated translocation across the cell envelope powered by ATP hydrolysis. Here we show that a more efficient paradigm is possible in Gram-positive bacteria where extracellular metal-free siderophores associate directly with apo-SBPs on the cell surface and serve as non-covalent cofactors



that enable the holo-SBPs to non-reductively extract ferric iron directly from host metalloproteins with so-called "ferrichelatase" activity. The resulting SBP-bound ferric siderophore complex is ready for import through an associated membrane permease and enzymatic turnover is achieved through cofactor replacement from the readily available pool of extracellular siderophores. This new "iron shuttle" model closes a major knowledge gap in microbial iron acquisition and defines new roles of the siderophore and SBP as cofactor and enzyme, respectively, in addition to the classically accepted roles as a transport substrate and receptor pair. We propose the formal name "siderophore-dependent ferrichelatases" for this new class of catalytic SBPs.

■ INTRODUCTION

Iron is an essential nutrient that must be scavenged by microbes, both commensals and pathogens, during colonization of mammalian hosts. 1,2 Bacteria have evolved several pathways to assimilate iron from common host sources including heme, ferritin, and transferrin.3 Common to all iron scavenging pathways is a need to import iron derived from extracellular iron sources across the bacterial cell envelope. A versatile means for accomplishing this is provided by the biosynthesis of siderophores, low-molecular-weight ferric iron chelators, and the co-expression of associated regulatory, efflux, receptor, and transport proteins.4 In Gram-negative bacteria this includes a TonB-dependent outer membrane receptor (OMR), a periplasmic siderophore-binding protein (SBP), and an ABC-type ATP-dependent permease. In Gram-positive bacteria, lack of an outer membrane precludes the need for an OMR, leaving only an extracellular membrane-anchored SBP and associated ABC permease to facilitate recognition and import, respectively.⁶ Continuous export of metal-free siderophores ensures a high-affinity reservoir for capturing extracellular ferric iron that can be distinguished by OMRs and SBPs in the form of a chiral ferric siderophore complex.

The functional roles of OMRs, SBPs, and ABC permeases in a variety of pathogen-specific siderophore systems have been firmly established through genetic and biochemical studies.^{5,6} In bacteria, siderophore-dependent iron uptake systems are under transcriptional control by the ferric uptake regulator (Fur).8 In Gram-negative bacteria, OMRs reversibly bind ferric siderophore complexes with nanomolar affinity first to an external "cork" domain and then to an internal "plug" domain.9 This two-site binding model is supported by X-ray crystal structures of OMRs with ferric siderophores bound to either the "cork" or "plug" domain separately, suggesting there is an orchestrated series of binding events and conformational changes leading up to translocation across the outer membrane. With assistance of the membrane-spanning TonB complex of proteins and energy from the proton gradient provided by ExbBD, 10 the ferric siderophore is imported to the periplasmic space,¹¹ presumably with a hand-off of the ferric siderophore from the OMR "plug" domain to the periplasmic SBP. 12 Interaction of the ferric SBP-siderophore complex with the ABC permease promotes import across the inner

Received: December 6, 2019 Published: March 9, 2020



membrane to the cytoplasm driven by ATP hydrolysis.¹³ In some instances, ferric iron is released in the periplasm via reduction where ferrous iron can be directly imported via the FeoABC complex.^{14,15} Alternatively, siderophore hydrolases can fragment the scaffolds of some siderophores, such as enterobactin, releasing lower affinity ferric chelation complexes.¹⁶ In Gram-positive bacteria, surface-displayed SBP lipoproteins bind ferric siderophores reversibly with nanomolar affinity and facilitate import to the cytoplasm via associated ATP-dependent membrane-embedded permeases.⁶ Ferrous iron can be released from some ferric siderophores, such as ferrichrome, in the cytoplasm via enzymatic reduction of the metal to provide unmodified metal-free siderophore, which can be recycled via efflux in certain bacteria.^{17,18}

Despite decades of research on siderophore-mediated iron acquisition in bacteria, there is still much to learn about the underlying molecular mechanisms governing import of ferric siderophore complexes. High-resolution X-ray crystal structures of siderophores bound to OMRs and SBPs have provided insight into siderophore scaffold recognition within the binding calyx, but the functional relevance of the observed states has not been fully investigated. ^{19,20} In the canonical transport model represented by the vitamin B_{12} transport pathway (BtuBCDF), a one-site binding model is proposed for the OMR, BtuB,²¹ and periplasmic binding protein, BtuF;²² thus, the molecule of vitamin B_{12} initially bound by the OMR (Gram-negative bacteria only) or periplasmic binding protein (all bacteria) is the molecule ultimately imported to the cytoplasm by the ABC permease, BtuCD. 13,23,24 For most transporters, this is a one-way trip, but for siderophores the ferric siderophore complex is imported and the metal-free siderophore is exported and recycled.¹⁷ This introduces the need to balance between import/export of two structurally related substrates, which mounting evidence suggests is achieved by a more complex membrane transport paradigm. 12,25,20

Raymond and co-workers performed stable isotope feeding studies with Ga(III) and Cr(III) siderophore complexes in model Gram-negative (Escherichia coli and Aeromonas hydrophila) and Gram-positive (Bacillus cereus) organisms that proved inconsistent with the canonical one-site binding and transport model for vitamin B_{12} . A follow-up study in Gram-positive bacteria demonstrated that recombinant variants of a soluble truncated SBP from B. cereus (YxeB) can directly promote the non-reductive exchange of ferric iron between hydroxamate siderophores.²⁶ Two working models for siderophore-mediated iron transport were proposed by Raymond and co-workers based on findings from these seminal studies (Figure 1). In the first model, referred to as the Raymond siderophore displacement model (Figure 1a), ²⁶ a metal-free siderophore initially bound to an OMR or SBP is "displaced" by a ferric siderophore that gains cell entry. This model fails to account for the likely scenario that metal-free siderophore concentration will be much higher than ferric siderophore concentration; thus, the SBP binding equilibrium will be dominated by metal-free siderophore under normal circumstances. In the second model, referred to as the Raymond iron shuttle model (Figure 1b),²⁶ ferric iron is "shuttled" from a ferric siderophore complex to a metal-free siderophore that ultimately gains cell entry. This model accounts for the higher concentration of metal-free siderophore dominating the SBP binding equilibrium but presents a new problem in that low ferric siderophore concentrations will

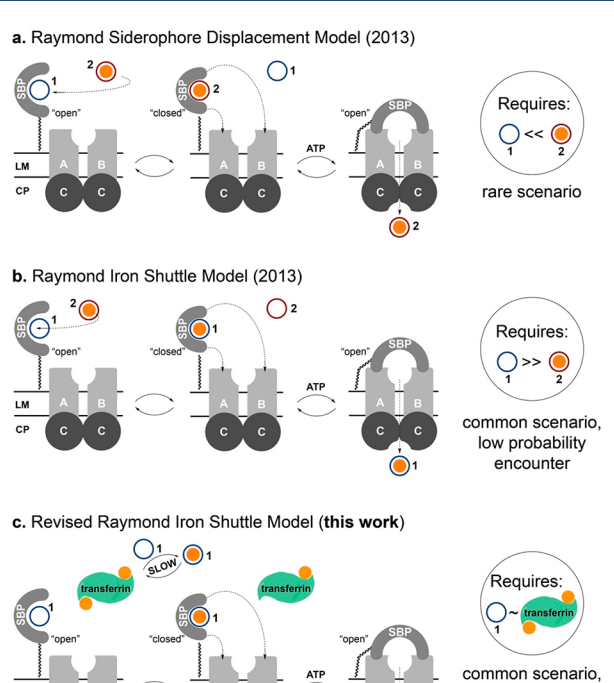


Figure 1. Schematic representation of the (a) Raymond siderophore displacement, (b) Raymond iron shuttle, and (c) revised Raymond iron shuttle (this work) models for siderophore-mediated iron import in Gram-positive bacteria. Siderophore displacement (a) is presumably only favored when the concentration of ferric siderophore is greater than metal-free siderophore, which is predicted to be a rare scenario. The original Raymond iron shuttle presumably requires a higher concentration of metal-free siderophore than ferric siderophore, which is common, but requires a rare chance encounter between both metal-free and ferric siderophores at the SBP. In this work, we present a revised model for the Raymond iron shuttle where SBPs catalyze the exchange of ferric iron from human transferrin, a more commonly encountered host iron source, to a bound siderophore cofactor. LM, lipid membrane; CP, cytoplasm; SBP, siderophore-binding protein.

high probability

encounter,

accounts for host Fe source

lead to a highly improbable encounter of both metal-free and ferric siderophores at the site of SBPs. The deficiencies of these two models presents a knowledge gap leading to the following question: What is the biological source of host iron? To fill this knowledge gap we considered the possibility that ferric transferrin, a common host iron source present during infections, could serve as the iron source where the SBP catalyzes iron exchange to the bound siderophore (Figure 1c).

At first, the benefit of employing an "iron shuttle" is not entirely clear until considering the biological source of iron; in this case, human transferrin. The direct exchange of iron between biological sources, such as transferrin (log $K_{\rm Fe}\approx 22$; 25 °C), 27 and high-affinity siderophores (log $K_{\rm Fe}\approx 32$; 25 °C) is predicted to be thermodynamically favorable ($K_{\rm eq}\approx 10^{10}$), but exceedingly slow at neutral pH ($t_{1/2}\sim$ weeks). 28 On the contrary, under acidic conditions (pH < 6.7), such as those at sites of advanced infection and inflammation, transferrin will readily lose iron that can be directly sequestered by siderophore present at the infection site. 28,29 Hence, there is a need for additional factors to provide a meaningful kinetic advantage for siderophore-mediated iron acquisition at the earliest stages of infection at neutral pH when nutrients are

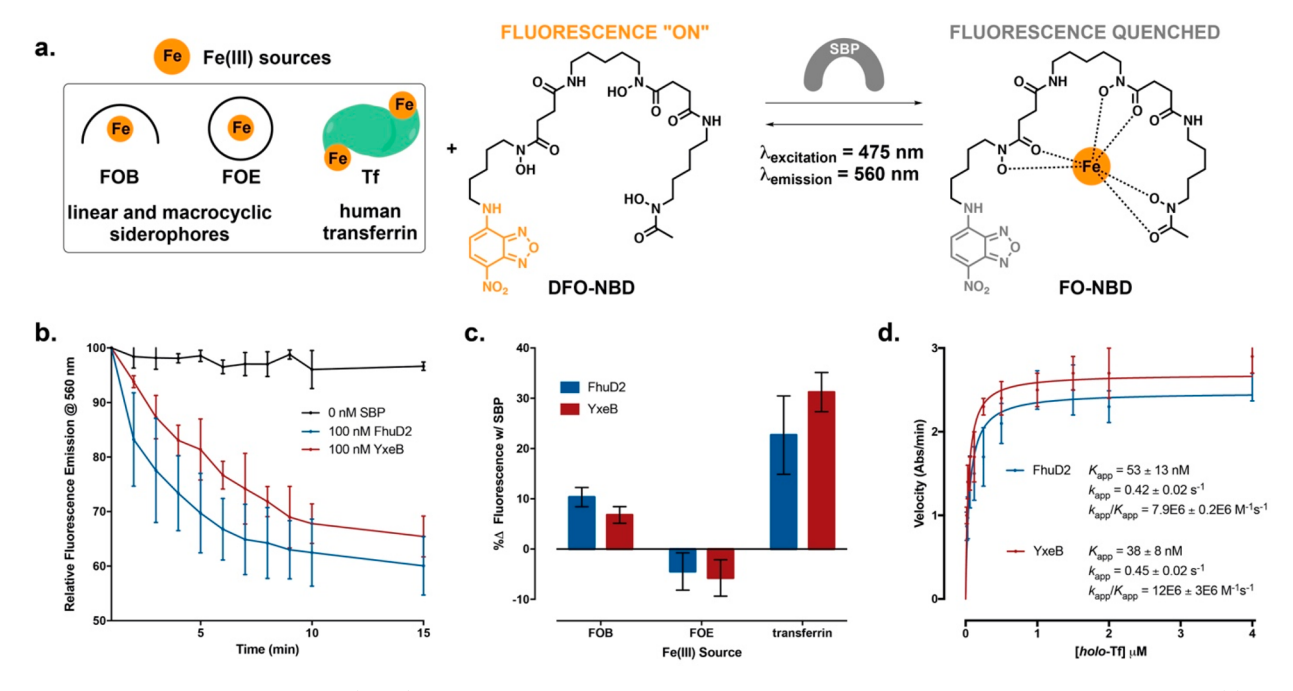


Figure 2. Siderophore-binding proteins (SBPs) catalyze the exchange of ferric iron from human transferrin to a siderophore cofactor. (a) General reaction scheme for the use of desferrioxamine-2-(4-nitro-2,1,3-benzoxadiazol-7-yl) conjugate (DFO-NBD) as a "turn off" fluorescent iron sensing probe that quenches upon chelation of iron(III). (b) Graph depicting relative fluorescence emission quenching of 2 μM DFO-NBD ($\lambda_{\text{excitation}}$ = 475 nm; $\lambda_{\text{emission}}$ = 565 nm) in the time domain using no SBP, 100 nM FhuD2, or 100 nM YxeB and 4 μM ferric human transferrin as the iron source. (c) Graph depicting the percentage change in the relative fluorescence emission of DFO-NBD ($\lambda_{\text{excitation}}$ = 475 nm; $\lambda_{\text{emission}}$ = 565 nm) after 15 min of incubation with 100 nM SBP (FhuD2 or YxeB) and 4 μM ferric iron source (FOB, FOE, or transferrin) relative to a control reaction with no added SBP. (d) Michaelis–Menten plot with apparent steady-state kinetic parameters for the exchange of ferric iron from variable transferrin to constant DFO-NBD (2 μM) catalyzed by 100 nM SBP (FhuD2 or YxeB). Error bars in all panels represent standard deviations for at least two independent trials.

scarce; this is a role filled by catalytic SBPs. Here, we demonstrate that metal-free siderophores serve as cofactors for SBPs, referred to from this point forward as holo-SBPs, to impart "ferrichelatase" activity to the otherwise non-catalytic SBPs. Siderophore-loaded holo-SBPs can rapidly extract ferric iron from biological sources at neutral pH, including human holo-transferrin, resulting in a non-reductive ferric iron exchange to the bound siderophore that presumably gains cell entry via the associated membrane permease. The concentration of extracellular metal-free siderophores far exceeds that of ferric siderophores shifting the binding equilibrium of SBPs toward the metal-free siderophore to seemingly prevent direct import of extracellular ferric siderophores. Our revised model accounts for this apparent contradiction in the membrane transport paradigm where the ferric siderophore complex is formed directly by the holo-SBP acting as a single-turnover catalyst that is regenerated by cofactor replacement from the extracellular pool of metal-free siderophores following import of the ferric siderophore.

In this work, we describe a fluorescence quenching assay for measuring steady-state iron exchange kinetics catalyzed by SBPs using a fluorescent siderophore probe. We probe the mechanistic basis of SBP-catalyzed iron exchange using a variety of linear and macrocyclic siderophore substrates and site-directed mutagenesis of amino acid residues in the SBP binding calyx. We establish that human ferric *holo*-transferrin interacts directly with bacterial SBPs and serves as an efficient iron-donating substrate for the non-reductive siderophore-dependent "iron shuttle" under neutral conditions. We have thus reimagined the Raymond iron shuttle model (Figure 1b,c) and further validated the occurrence of the Raymond

siderophore displacement (Figure 1a) membrane transport paradigms *in vitro* by establishing the surprising multifaceted roles of the SBP and siderophore as catalyst/receptor and cofactor/transport substrate, respectively. We propose a new name for this class of catalytic SBPs—"siderophore-dependent ferrichelatases".

■ RESULTS AND DISCUSSION

Model SBP Systems from Gram-Positive Pathogens.

In Gram-positive bacteria, SBPs are exported across the cytoplasmic membrane and anchored to the extracellular face of the lipid membrane where they are free to associate with an ABC-type membrane permease. The original "iron shuttle" and "siderophore displacement" models proposed by Raymond were based on studies involving a truncated SBP from B. cereus, YxeB, lacking the peptide signal sequence. 25,26 YxeB is part of the ferric hydroxamate siderophore uptake (Fhu) system including the permease that enables B. cereus and related species to scavenge hydroxamate xenosiderophores from local environments.³⁰ A homologous Fhu system exists in many Gram-positive bacteria, including human pathogenic Staphylococcus aureus. 31,32 We sought to validate these siderophore transport models using YxeB as in the Raymond studies and extend the findings to a homologous SBP, FhuD2, in the human pathogen S. aureus.

Pathogenic strains of *S. aureus* typically produce the endogenous siderophores staphyloferrin A/B and the general metallophore staphylopine.^{32–36} The biosynthetic genes and associated transport genes for the staphyloferrins and staphylopine have been investigated biochemically and implicated in pathogen virulence.^{37–41} Curiously, genes associated with the

Table 1. Apparent Binding Affinities and Kinetic Parameters for YxeB, FhuD2, and Variants

				app $K_{\rm d}$ (nM)			
SBP	app $K_{\rm m}$ (nM)	app k_{cat} (s ⁻¹)	app $k_{\rm cat}/K_{\rm m}~(\times 10^6~{\rm M}^{-1}~{\rm s}^{-1})$	transferrin	DFOB	FOB	FOE
YxeB	40 ± 10	0.5 ± 0.02	10 ± 3	100 ± 40	30 ± 20	50 ± 30	30 ± 9
FhuD2	50 ± 10	0.4 ± 0.02	8 ± 0.2	70 ± 30	90 ± 10	30 ± 6	50 ± 6
Y256F	150 ± 30	0.4 ± 0.01	2 ± 0.5	70 ± 9	80 ± 30	60 ± 10	40 ± 20
Y106F	80 ± 10	0.3 ± 0.01	4 ± 0.5	100 ± 10	80 ± 20	40 ± 8	80 ± 10
R175A	220 ± 50	0.3 ± 0.02	1 ± 0.3	110 ± 30	40 ± 9	30 ± 9	50 ± 20
W255A	350 ± 110	0.3 ± 0.02	0.6 ± 0.2	110 ± 80	60 ± 20	60 ± 50	30 ± 9
Y254F	40 ± 10	0.2 ± 0.01	6 ± 0.8	90 ± 20	50 ± 10	10 ± 2	20 ± 3
Y167F	50 ± 20	0.2 ± 0.01	3 ± 1	80 ± 20	60 ± 9	40 ± 6	30 ± 3
Y169F	50 ± 20	0.1 ± 0.01	2 ± 1	110 ± 20	70 ± 10	40 ± 9	20 ± 2
W173A	50 ± 10	0.03 ± 0.002	0.9 ± 0.1	140 ± 30	100 ± 50	60 ± 8	90 ± 30

^aAll error values represent standard deviations for at least two independent trials.

Fhu xenosiderophore transport system (FhuABCD1D2) are also required for full pathogen virulence despite lacking associated biosynthetic genes to ensure the hydroxamate substrates will be present during infection. 31,42,43 This led us to hypothesize that there might be additional roles for the Fhu gene products in pathogen virulence. This hypothesis is supported by the observation that antibodies targeting the SBP FhuD2 are protective against S. aureus infections; a finding that led Novartis to develop vaccine candidates for MRSA based on FhuD2-targeting antibodies.⁴³ Interestingly, there are two SBPs in the Fhu operon-FhuD1 and FhuD2. Knockout studies proved that FhuD2, but not FhuD1, is required for pathogen virulence in vivo suggesting that FhuD2 is the only functional SBP. 43-45 Furthermore, the appearance of spontaneous resistance to salmycin, a natural ferrioxamine antibiotic conjugate from Streptomyces violaceus, arises from mutations in the fhud2 gene resulting in truncation or transcriptional disruption of FhuD2, leaving FhuD1 unchanged. 46,47 Collectively, these findings suggest that FhuD1 is not a functional substitute for FhuD2. 45 Hence, we focused on elucidating the role of FhuD2 in the "iron shuttle" and "siderophore displacement" paradigms.

Development of a Fluorescent Probe for Measuring **Fe Exchange.** In order to study the siderophore "iron shuttle" model, we developed a kinetic assay for measuring the rates of iron exchange between two ligands. Classically, this type of assay has been achieved via competitive chelation experiments using optical absorbance or fluorescence-based approaches when the two chelators have unique spectral properties. ^{7,48,49} Here, an analytical method was needed to distinguish between two ferrioxamine siderophore chelators, which have no inherent fluorescence and identical optical absorbance spectral properties (Figure S1). Thus, we leveraged a previously described fluorescent ferrioxamine siderophore derivative, 7nitrobenz-2-oxa-1,3-diazole-desferrioxamine B (DFO-NBD), originally developed to monitor iron distribution in plants. The fluorescence of DFO-NBD was reported to rapidly quench upon chelation of ferric iron.⁵⁰ We envisioned using this fluorescence quenching property of DFO-NBD as a "turnoff" fluorescent probe against a variety of iron donor molecules (ferric siderophore and transferrin complexes) in the presence or absence of SBPs (FhuD2 and YxeB), the putative "ferrichelatases" catalyzing iron exchange (Figure 2a).

The DFO-NBD conjugate was easily prepared via nucleophilic aromatic substitution of 4-chloro-7-nitrobenz-2oxa-1,3-diazole (NBD-Cl) by the free desferrioxamine B (DFOB) primary amine under mildly basic conditions (Figure

S2).50 As expected, DFO-NBD formed a 1:1 complex with ferric iron (FO-NBD; apparent log $K_{\rm Fe} = 30.8 \pm 0.3$) with similar apparent stability as the ferric complex (FOB; apparent $\log K_{\rm Fe} = 30.3 \pm 0.4$) derived from the parent DFOB siderophore (Figure S3). The fluorescence emission spectrum of DFO-NBD produced a distinct band spanning ~540-580 nm ($\lambda_{\text{emission}} = 560 \text{ nm}$), corresponding to excitation at 475 nm $(\lambda_{\text{excitation}})$ (Figure S4). As previously reported, 50 the fluorescence emission was quenched by addition of FeCl₃ and analysis of the titration curve was consistent with the formation of a 1:1 siderophore:iron(III) complex. We next introduced a variety of iron donors and monitored this fluorescence quenching in the time domain for kinetic measurements.

Development of a Kinetic Fe Exchange Assay. With a functional chemical probe for measuring iron exchange in hand, we investigated the ability of SBPs to enhance the relative rate for iron exchange from a ferric iron donor substrate to the DFO-NBD fluorescent probe. We expressed and purified truncated variants of the ferric hydroxamate SBPs YxeB and FhuD2 from B. subtilis and S. aureus, respectively, that replace the N-terminal signal peptide sequence with an Nterminal hexahistidine motif (Figure S5; Tables S1 and S2).51,52 We used an intrinsic Trp fluorescence quenching binding assay to confirm that both DFO-NBD and FO-NBD bind to FhuD2 and YxeB with nanomolar affinity (Table 1, Figure S6). The fluorescence emission response of DFO-NBD was linear in the concentration ranges used in iron exchange assays (Figure S7a). The fluorescence emission of DFO-NBD was somewhat enhanced in the presence of SBPs (Figure S7b). We chose the linear trihydroxamate siderophore ferrioxamine B (FOB), the macrocyclic trihydroxamate siderophore ferrioxamine E (FOE), and human holo-transferrin (holo-Tf) as ferric iron donor substrates (Figure S1). We confirmed by intrinsic Trp fluorescence quenching that all ferric siderophores, metal-free siderophores, and holo-Tf were bound by FhuD2 and YxeB with nanomolar affinity (Table 1, Figure S6).

The basic idea for measuring iron exchange kinetics was to bias the equilibrium by starting with 100% of the ferric iron complexed with the donor substrate in the presence or absence of SBP (Figure 2a). The reaction was then initiated by addition of the probe DFO-NBD with continuous monitoring of fluorescence emission ($\lambda_{\text{excitation}} = 475 \text{ nm}$; $\lambda_{\text{emission}} = 560 \text{ nm}$), which decays over time with exchange of ferric iron from the donor substrate to DFO-NBD forming metal-free substrate and FO-NBD (Figure 2b). Fluorescence quenching data at a given time point was interpreted as the percentage change in

fluorescence relative to a control sample lacking a ferric iron donor substrate and containing DFO-NBD and SBP at the concentrations specified for a given experiment (Figure 2c). As the reaction progresses, back exchange of ferric iron from FO-NBD to metal-free substrate and homo exchange to DFO-NBD gave the appearance of feedback inhibition. Since the initial equilibrium was biased with 100% ferric donor substrate, we assumed that initial rates represented steady-state kinetics for iron exchange to DFO-NBD (Figure 2d). We optimized the assay for the concentrations of SBP (100 nM) and substrates (low μ M) to reflect biologically relevant concentrations without oversaturation (Figures S7 and S8). We used this kinetic assay to determine if SBPs are true catalysts that shuttle ferric iron from a donor substrate to a bound metal-free siderophore.

SBPs Are Siderophore-Dependent Ferrichelatases. According to the nomenclature proposed by Berntsson et al., 53 SBPs belong to the type IIA subgroup of substratebinding protein superfamily. This class of SBPs are exclusively associated with ABC permeases with a cradle-like structure formed between the N- and C-terminal globular domains joined by a rigid α -helix. The region between the two globular domains forms a distinct hydrophobic binding calyx with conserved residues that form hydrogen-bonding contacts with the oxophilic hydroxamate, catecholate, and α -hydroxycarboxylate ligands found in most siderophore scaffolds.⁵⁴ SBPs bind siderophores and associate with membrane permeases to facilitate siderophore translocation. 13,23,24 Catalytic roles for SBPs have largely been overlooked although the emergence of catalysis has been well documented for related substratebinding proteins including chalcone isomerase⁵⁵ and cyclohexene dehydratase,⁵⁶ which both catalyze first-order isomerization reactions using a single binding site for stabilizing the reaction transition state. We hypothesized that the SBPs FhuD2 and YxeB might have similarly emerged as iron transfer catalysts via a single-binding site model where siderophore binding pre-organizes hydroxamate ligands to receive ferric iron from a donor substrate; this is analogous to the classic "ferrochelatase" activity where ferrous iron is non-reductively transferred to a bound heme cofactor. 57-59 Here, the terms "ferrochelatase" and "ferrichelatase" refer to enzymes that insert ferrous or ferric iron, respectively, into a ligand by catalyzing ligand exchange without oxidation or reduction of the metal center.

By the principle of microscopic reversibility, SBPs with ferrichelatase activity should catalyze the forward and reverse reactions of iron exchange to establish equilibrium between two siderophores where the equilibrium constant is determined by the apparent iron affinity constants of each siderophore. We probed the ability of FhuD2 and YxeB to catalyze this type of iron exchange using linear (FOB) and macrocyclic (FOE) siderophore donors of ferric iron. Use of linear FOB as ferric iron donor provided up to 10% relative fluorescence quenching of DFO-NBD in the presence of SBPs, while macrocyclic FOE had the opposite effect of increasing relative fluorescence up to 10% compared to the no SBP control (Figures 2c, S9, and S10). We attributed this to the ability of linear FOB to serve as a donor of ferric iron, while macrocyclic FOE was unable to serve as an iron donor. We found this to be a general trend also observed for the related linear and macrocyclic ferric siderophore complexes danoxamine (DanFe) and danoxamine macrolactone (DanMFe) (Figures S11-S13). For linear siderophore iron donors, the

relative rate of iron exchange was dependent on time and the concentration of both substrates and SBP, consistent with a steady-state model for ferrichelatase activity (Figure S8).

Linear, but Not Macrocyclic, Siderophores Are Iron **Donors.** The SBP-catalyzed exchange of iron between siderophores was independent of the apparent binding affinity for ferric iron (log K_{Fe}). FO-NBD is a linear siderophore with an apparent log $K_{\rm Fe}$ (30.8 \pm 0.3) similar to FOB (30.3 \pm 0.4) and greater than DanFe (27.8 ± 0.3);⁵¹ both are linear siderophores that serve as iron donor substrates for FhuD2 and YxeB (Figures 2c, S11-S13). This observation supports a kinetic role for the SBP in speeding up the rate of iron exchange, which is exceedingly slow in the absence of SBP. Similarly, the failure of macrocyclic siderophores, FOE (log K_{Fe} = 32.4 \pm 0.1) and DanMFe (log K_{Fe} = 25.4 \pm 0.1),⁵¹ to serve as iron donors was independent of apparent iron affinity. Given that metal-free siderophores are predicted to be at a much higher concentration than ferric siderophores, which inhibits SBP ferrichelatase activity, we considered the possibility that direct iron exchange between siderophores might not be a biologically relevant iron shuttle. Therefore, we turned our attention to more biologically relevant iron donor substrates such as human holo-Tf, which is overproduced at the site of infection.^{3,4}

Human Holo-Transferrin Is an Efficient Iron Donor. When using holo-Tf as the ferric iron donor substrate for the DFO-NBD/SBP iron exchange assay we observed a more pronounced fluorescence quenching effect compared to sideropohore iron donors with up to 35% fluorescence quenching relative to a control lacking SBPs (Figures 2d and S14). The iron exchange was dependent on the concentrations of holo-Tf, SBPs, and DFO-NBD consistent with fluorescence quenching by formation of FO-NBD resulting from ferrichelatase activity of SBPs (Figures S8 and S14). We also prepared an untagged version of FhuD2 to demonstrate that the N-terminal-His6 tag was not responsible for promoting the iron exchange. Cleavage of the tag with thrombin provided the untagged FhuD2 in high purity (Figure S15a). Evaluation of the untagged and His6-tagged FhuD2 variants using 4 µM holo-Tf and 2 µM DFO-NBD gave nearly identical fluorescence decay plots (Figure S15b). Under the same conditions, we also measured the fluorescence decay promoted by 100 nM N-His₆tagged FhuD2 in the presence of 50 nM NiCl₂ to presumably form the 2:1 His₆-Ni(II) complex of FhuD2 and observed very similar plots as experiments lacking Ni. Given that carbonate is the accepted biological ligand for the ferric center of transferrin,²⁹ we showed that 25 mM NaHCO₃ had no apparent effect on the FhuD2-catalyzed exchange of iron from holo-Tf to DFO-NBD (Figure S15c). We next determined Michaelis-Menten steady-state kinetic parameters for FhuD2 and YxeB under saturating DFO-NBD and variable holo-Tf. Both FhuD2 and YxeB produced similar apparent K_m values for holo-Tf of 53 \pm 13 and 38 \pm 8 nM, respectively, and apparent k_{cat} values (~0.4 s⁻¹) resulting in similar overall catalytic efficiencies (Figure 2d). The apparent K_m values were consistent with the apparent K_d values measured via intrinsic tryptophan fluorescence quenching, 70 ± 30 and 100 ± 40 nM, respectively (Table 1, Figure S6). Both methods suggest that FhuD2 and YxeB interact with holo-Tf at nanomolar concentrations. The nature of this binding interaction remains unclear, but seems to be transient in nature since pull-down experiments have failed to reveal stable SBP-Tf complexes. In the related maltose binding protein system, ligand binding and

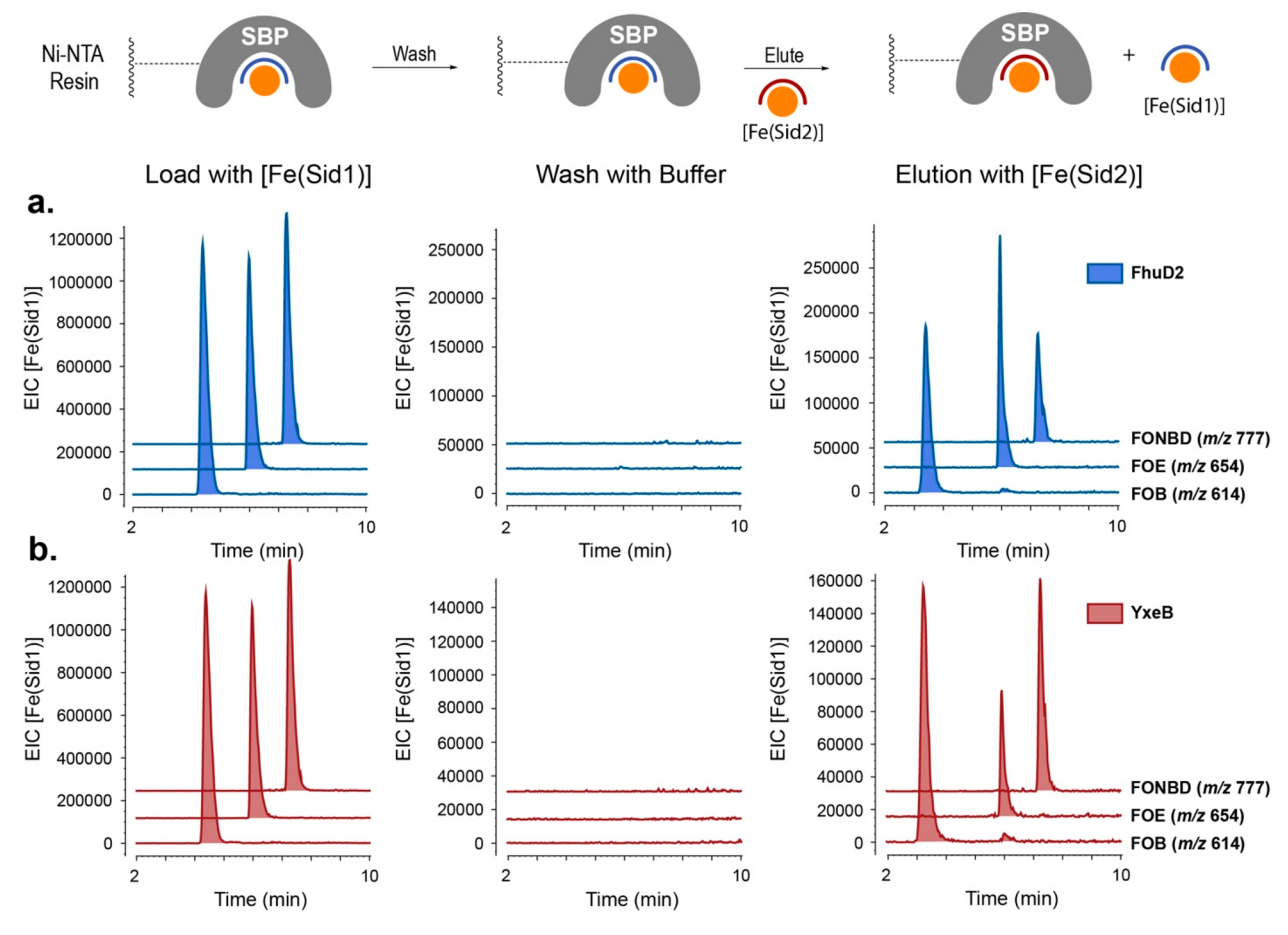


Figure 3. Ferrioxamine siderophores (FOB, FOE, and FONBD) bind reversibly and competitively to resin-immobilized FhuD2 and YxeB Siderophore binding proteins from *S. aureus* and *B. subtilis*, respectively. N-His $_6$ -FhuD2 (a) or N-His $_6$ -YxeB (b) was immobilized on Ni-NTA resin and loaded with a mixture of siderophores [Fe(Sid1)] (FOB, FOE, and FONBD), washed with phosphate buffer, and eluted with [Fe(Sid2)] (SFOB). Column elutions were analyzed by LC-MS for each siderophore component in the load [Fe(Sid1)] (m/z = 614, 654, and 777 for FOB, FOE, and FONBD [M+H]⁺ ions, respectively). Extracted ion chromatograms (EIC) are shown for FOB, FOE, and FONBD. EICs are representative for at least two independent trials.

protein molecular crowders were both shown to favor the closed conformation, which might also play a role here in Tf-binding. We further probed the nature of the SBP—Tf interaction by dissecting the role of siderophores as required cofactors for SBP ferrichelatase activity.

Siderophores Are Cofactors and Transport Substrates. In our model of the siderophore iron shuttle, the siderophores serve a dual purpose as cofactor for a SBP ferrichelatase and transport substrate for an associated ABC permease (Figure 1c). Reversible siderophore binding is key for achieving this dual role. We validated that FhuD2 and YxeB bind reversibly to the linear (FO-NBD and FOB) and macrocyclic ferric siderophores (FOE) using affinity chromatography. 52 The N-His₆-tagged SBPs were immobilized on Ni-NTA resin and loaded with an equimolar mixture of FO-NBD, FOB, and FOE (Figure 3). Treatment of the SBP resin with a fourth ferric siderophore, succinylferrioxamine B (SFOB), resulted in the release of all three bound siderophores as detected by LC-MS. According to this reversible binding model, there will be a competition for SBP binding in the extracellular space between metal-free and ferric siderophores. Since the concentration of metal-free siderophore is anticipated to be much greater than ferric siderophores, the binding equilibrium will favor the metal-free siderophore. It is unclear if metal-free siderophores are readily transported into cells, but

there is clear evidence that metal-free siderophores can compete with ferric siderophores for cell entry via SBP-associated pathways. Presumably, there will be a gating mechanism at play by the ABC permease that enables selective import of ferric siderophores over metal-free siderophores. Thus, we propose that metal-free siderophores will stay bound to SBPs displayed on the cell surface, acting as cofactors for the now *holo-SBPs* to impart ferrichelatase activity that enables the stripping of iron from biological sources of ferric iron including *holo-Tf*.

To further support this model, we performed iron exchange assays with FhuD2 between *holo*-Tf and DFO-NBD in the presence of increasing concentrations of a competing metal-free siderophore DFOB (Figures 4a and S16). Increasing concentrations of DFOB were inhibitory toward the time- and FhuD2-dependent quenching of DFO-NBD fluorescence. Competing DFOB can displace DFO-NBD from FhuD2 and serve as the siderophore cofactor and acceptor of ferric iron from *holo*-Tf; thus, blocking the formation of FO-NBD and associated quenching of DFO-NBD fluorescence. We confirmed that DFOB can serve as the iron acceptor using LC-MS. Analysis of the iron exchange assay between DFOB and *holo*-Tf catalyzed by FhuD2 by LC-MS revealed an order of magnitude increase in ion counts for FOB relative to a control reaction lacking FhuD2 (Figures 4b and S16). This LC-MS

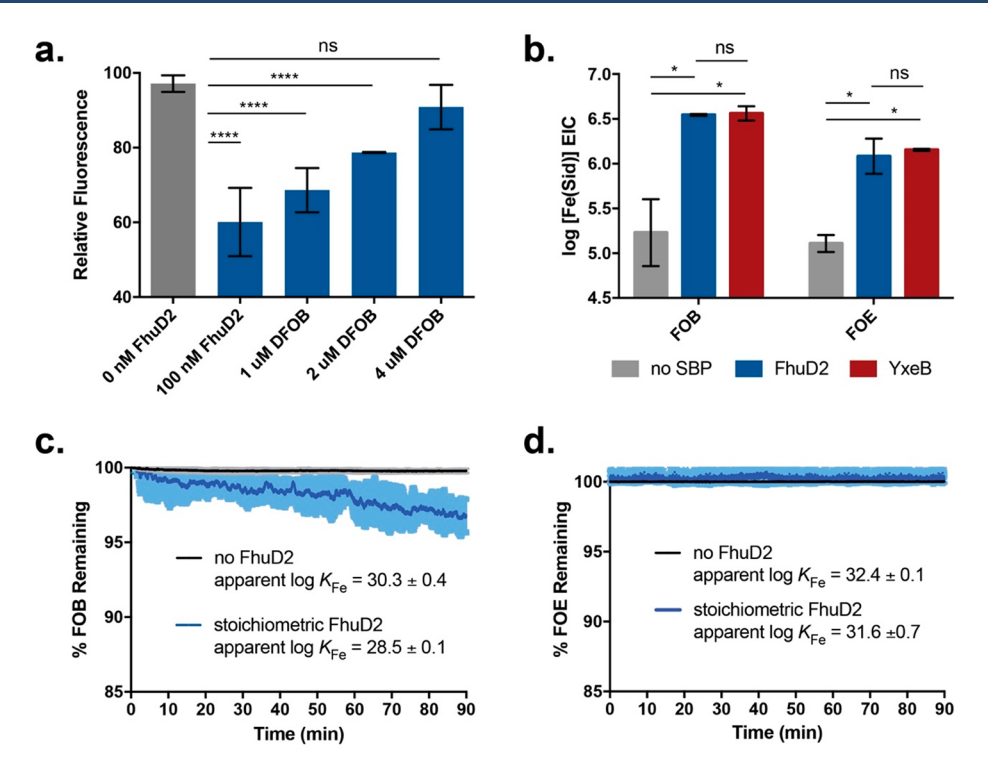


Figure 4. Macrocyclic siderophores can accept, but not donate, ferric iron during SBP-catalyzed exchanges. (a) Graph depicts the relative fluorescence emission quenching of 2 μ M DFO-NBD ($\lambda_{\rm excitation}=475$ nm; $\lambda_{\rm emission}=565$ nm) after 60 min of incubation with 100 nM FhuD2, 2 μ M ferric transferrin, and variable concentrations of competing DFOB (0–4 μ M). (b) Graph depicts the log of extracted ion counts (EICs) for [Fe(Sid)] complexes, FOB or FOE, after treatment of 50 μ M DFOB or FOE, respectively, with 50 μ M ferric transferrin without or with 10 μ M SBP (FhuD2 or YxeB). All EICs were normalized to a quinoline internal standard. The graphs in panels (c) and (d) depict the relative percentage of (c) FOB or (d) FOE remaining after treatment with 1.2 equiv of EDTA in the presence or absence of stoichiometric FhuD2. Siderophore concentrations were determined by optical absorbance at 427 nm. The apparent ferric iron affinity (log $K_{\rm Fe}$) was calculated from the decay plots. Error bars in all panels represent standard deviations for at least two independent trials. The shaded regions above the curve in panels (c) and (d) represent the error bars for every single data point along the continuously recorded data set; *****p < 0.001; *p < 0.05; ns = not significant.

method confirms that our fluorescence-based assay for iron exchange using DFO-NBD is a valid method to quantify SBP ferrichelatase activity.

Macrocyclic Siderophores Are Iron Acceptors. Results from the LC-MS studies inspired us to reconsider the role of macrocyclic siderophores in the bacterial iron shuttle. Given that macrocyclic siderophores cannot serve as iron donors, we hypothesized that macrocyclic siderophores can only serve as the iron acceptor. An exclusive role as iron acceptor fits our model for SBPs as siderophore-dependent ferrichelatases and makes sense given that metalloproteins such as holo-Tf are more prevalent than ferric siderophores during early stages of infection.³ Indeed, macrocyclic DFOE was able to serve as a ferric iron recipient from donor holo-Tf in the FhuD2catalyzed iron exchange reaction at neutral pH. Similar to the outcomes of reactions with linear DFOB as the iron acceptor, LC-MS analysis of the reaction mixture indicated an order of magnitude greater ion counts for macrocyclic FOE compared to reactions lacking the FhuD2 ferrichelatase (Figures 4b and S17). Enhanced ligand pre-organization and rigidity give macrocyclic siderophores higher relative log K_{Fe} values than linear counterparts providing more thermodynamic driving force for the SBP-catalyzed iron exchange from holo-Tf. This gives credence to the large number of macrocyclic siderophores and other siderophore scaffolds that efficiently pre-organize sets of the multidentate ligands to chelate ferric iron.

The ability of SBPs such as FhuD2 and YxeB to utilize a wide range of xenosiderophores as cofactors and transport substrates seems like a positive evolutionary trait since microbes can never be sure of xenosiderophore availability in a given environment. 30,51,61 Hydroxamates are common chelating groups in siderophores; thus, it is beneficial to express xenosiderophore utilization pathways for this ubiquitous class of metabolites.7 Indeed, hydroxamate siderophore production occurs within the human microbiome providing the SBP cofactor to both commensals and pathogens.² The hydrophobic binding calyx and high degree of inherent conformational flexibility enables SBPs to bind structurally diverse siderophores. SBPs adopt "closed" and "open" conformational states associated with docking to the permease and release of substrate during import, respectively. 13,21-24 The dynamic conformational flexibility of SBPs might influence the kinetic and thermodynamic stability of a bound ferric siderophore complex. 56,64 Flexible linear siderophore ferric iron complexes are predicted to be more strongly influenced by SBP conformational dynamics than more rigid macrocyclic siderophores. This hypothesis is consistent with our observation that linear siderophores can serve as iron donors and acceptors while macrocyclic siderophores can only serve as acceptors.

To test the thermodynamic aspect of our hypothesis, we measured the apparent thermodynamic ferric iron stability constant (log $K_{\rm Fe}$) of linear FOB and macrocyclic FOE while in a 1:1 stoichiometric complex with FhuD2. The FOB:FhuD2

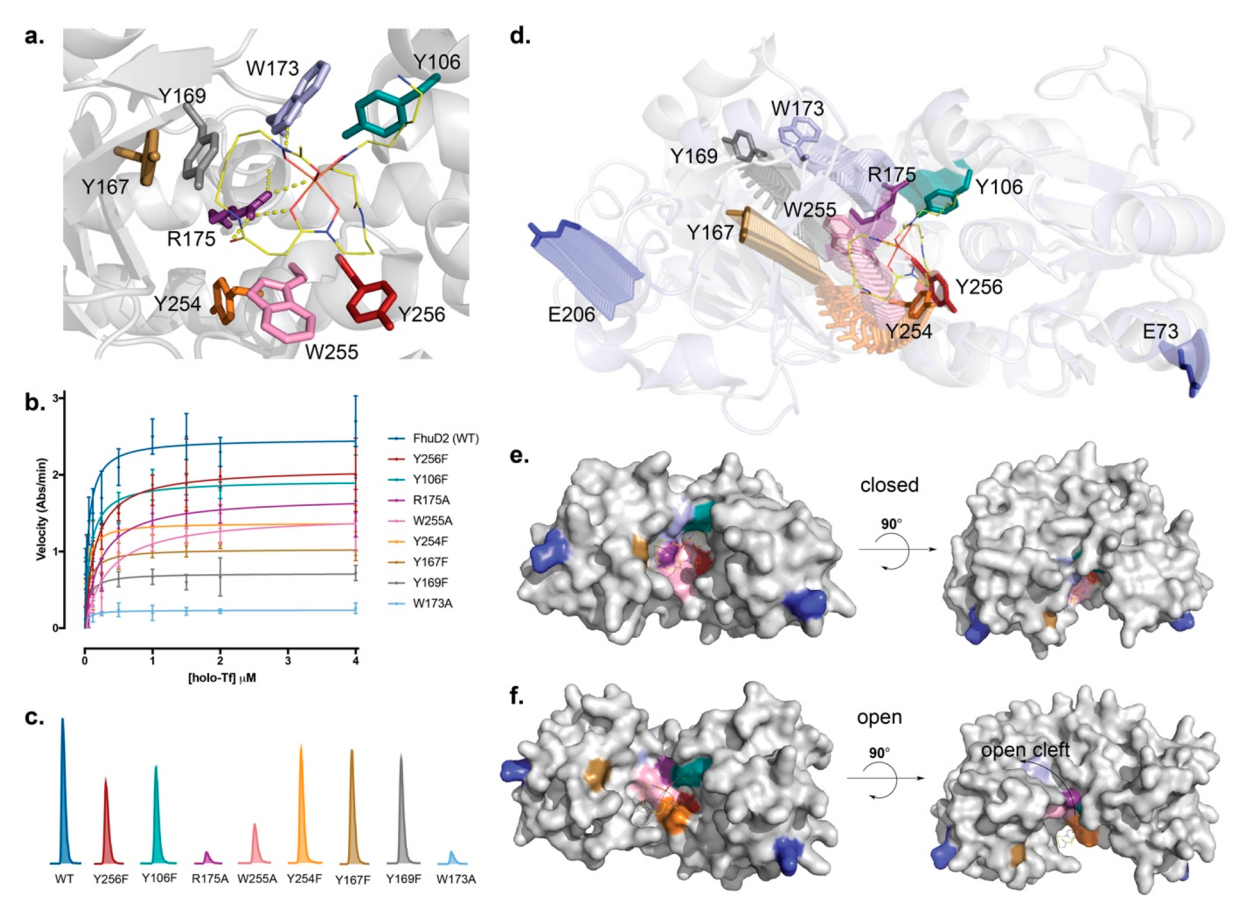


Figure 5. Mutational scanning of FhuD2 reveals active site residues involved in substrate binding and catalysis. (a) Active site residues in FhuD2 that were mutated. Color-coding of residues matches data sets in all panels. (b) Michaelis—Menten plot for wild-type and mutant FhuD2 variants (100 nM) reveals saturation kinetics for ferric transferrin and apparent changes in v_{max} for the exchange of ferric iron to 2 μ M DFO-NBD. (c) Relative binding and displacement of FOB to wild type and mutant FhuD2 variants. N-His₆-FhuD2 variant was immobilized on Ni-NTA resin and loaded with FOB, washed with phosphate buffer, and eluted with SFO. Column elutions were analyzed by LC-MS for FOB (m/z = 614 for [M +H]+). Extracted ion chromatograms (EIC) are shown for FOB and were normalized to a quinoline internal standard. EICs are representative for at least two independent trials. (d) Stacked-state model of the transition from "open" (dark, opaque residues) to "closed" (transparent residues) for FhuD2 highlighting residue dynamics. Panels (e) and (f) show surface models for FhuD2 in the (e) "closed" and (f) "open" states revealing a cleft from the movement of Y167, Y169, and W173. Images in panels (a) and (d)–(f) were generated using PyMOL v2.2 (Schrödinger, Inc.). The stacked-state model in panel (d) was generated using the morph function in PyMOL. The "closed" and "open" states of FhuD2 were generated from PDB entries 4fil and 4fna, respectively. Error bars in panel (b) represent standard deviations for at least two independent trials.

complex produced an apparent log $K_{\rm Fe}$ value (28.5 \pm 0.1) that was 2 orders of magnitude lower than the parent FOB without FhuD2 present (30.3 \pm 0.4) (Figure 4c). We observed the same trend for the linear siderophore DanFe (Figure S18). Notably, the FOE:FhuD2 complex gave the same apparent $\log K_{\rm Fe}$ value (31.6 \pm 0.7) as the parent FOE without FhuD2 present (32.4 ± 0.1) within the margin of error (Figure 4d). These observations suggest that ferric iron complexes derived from flexible linear ferrioxamine siderophores are destabilized within the binding calyx of SBPs, while rigid macrocyclic siderophores are unaffected. This is consistent with the hypothesis that conformational flexibility of SBPs can be transferred to flexible ligands, which has been demonstrated discretely for a variety of enzymes that employ substrate conformational control to stabilize reaction transition states (Figure S19). 55,56 Notably, the apparent log $K_{\rm Fe}$ of both linear and macrocyclic siderophores when bound to FhuD2 remain higher than that of holo-Tf ensuring favorable thermodynamics for the iron shuttle.

Calyx Residues Are Required for Cofactor Binding and Catalysis. The siderophore binding calyx in FhuD2 and

YxeB is mostly lined with hydrophobic aromatic residues (Trp, Tyr, Phe). Crystal structures of FhuD2 bound to FOB show that conserved residues including Trp173 and Arg175 make hydrogen-bonding interactions with two of the three hydroxamate ligands in the octahedral coordination sphere of the ferric iron center.⁶³ No direct interaction between FhuD2 residues and the ferric metal center have been observed, which distinguishes FhuD2 and related SBPs from known ferric iron binding proteins (FBPs). 54,65 However, a related SBP, CeuE from Campylobacter jejuni, has been shown to partially fill the octahedral ferric iron coordination sphere of some bis- and mono-catecholate ferric iron siderophore complexes using Tyr and His donating ligands. 66 We could measure apparent FeCl₃ binding affinities of 56 \pm 8 nM and 115 \pm 55 nM for FhuD2 and YxeB, respectively, but the formation of a stable or transient SBP-iron(III) needs further validation (Figure S6). This led us to pursue site-directed mutagenesis of FhuD2 in order to identify calyx residues that are potentially involved in siderophore binding, metal binding, and the chemical steps of iron exchange during catalysis.

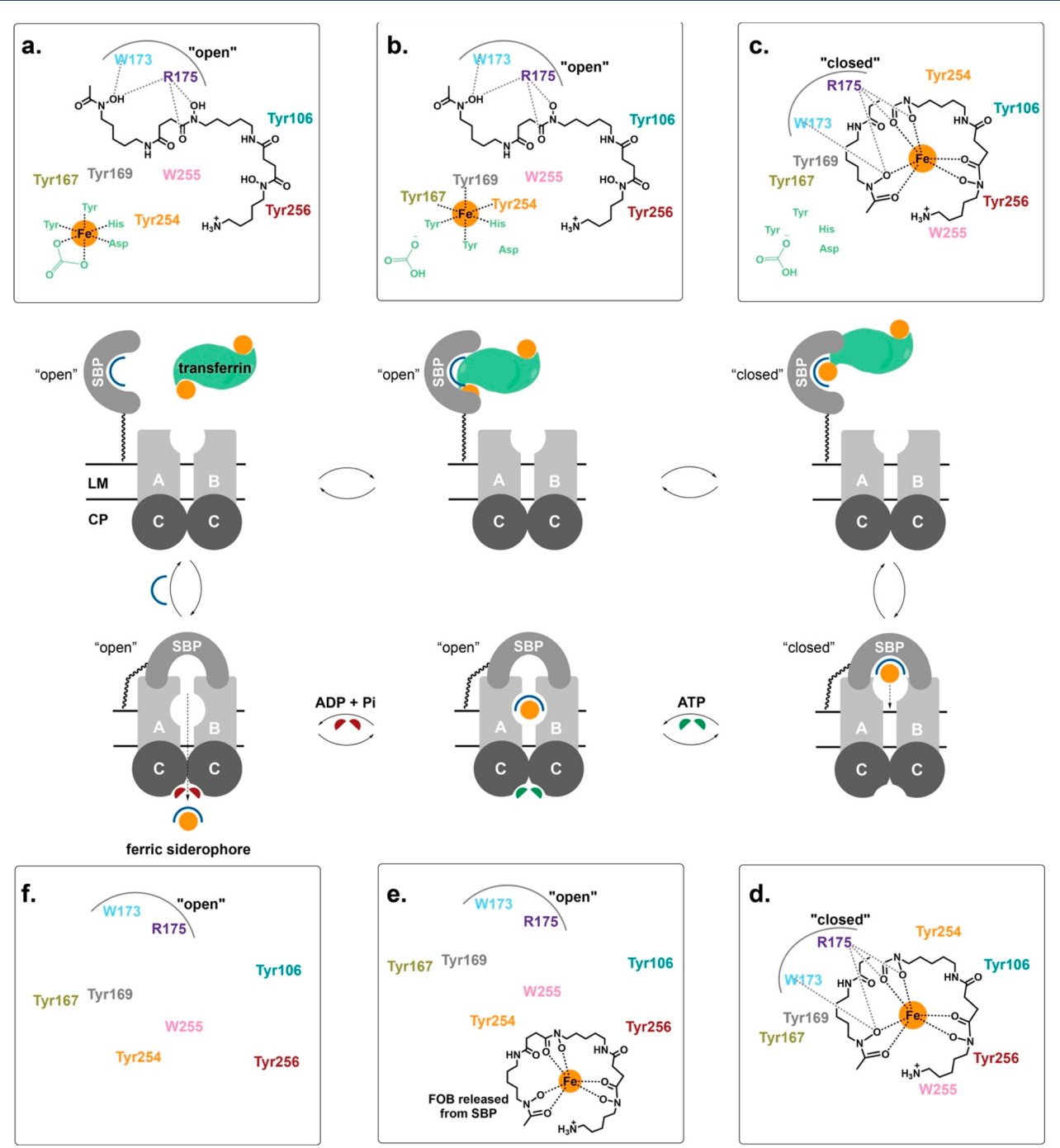


Figure 6. Mechanistic model for the siderophore-dependent ferrichelatase catalytic cycle. Shown is iron exchange from an octahedral ferric iron source (transferrin is shown here) to a siderophore cofactor (DFOB is shown here) bound to a SBP (shown here is FhuD2). (a) Resting state of membrane-anchored SBP with bound DFOB in the "open" state. (b) Interaction of DFOB-bound SBP in the "open" state with ferric transferrin (Tf) leading to ligand exchange of the carbonate and Tf-Asp residue by Tyr167, Tyr169, and Tyr254 of the SBP to form a transient mixed SBP-Tf ferric complex. (c) Transition to the "closed" SBP conformation with ligand exchange to DFOB hydroxamates leading to form the thermodynamic octahedral FOB ferric complex. (d) Dissociation of *apo-*Tf allowing for association of the "closed" FhuD2-FOB complex with the surface exposed region of the ABC permease to promote ATP binding by the cytoplasmic ATPase domains. (e) Transition to the "open" SBP conformation moves W255 into the binding calyx releasing FOB into the permease transmembrane helix cavity. (f) Hydrolysis of ATP to ADP and P_i by the ATPase domain drives FOB import to the cytoplasm. The ferric transferrin chelation model is based on the X-ray crystal structure of the N-terminal lobe of human serum transferrin with a bound carbonate ligand (PDB 1a8e). Calyx residue placement and numbering is based on the X-ray crystal structures of FhuD2 bound to FOB in the "closed" conformation (PDB 4fil) and *apo-*FhuD2 (PDB 4fna).

Previous whole cell studies of FhuD2 mutations in *S. aureus* growth assays revealed some calyx residues that might be involved in siderophore utilization.⁶⁷ We analyzed these residues in reference to the published X-ray structure of the "closed" FhuD2 conformation bound to FOB (Figure 5e) and

the published NMR structure of *apo*-FhuD2 in the "open" conformation (Figure 5f) to identify residues in the binding calyx close to FOB and residues that undergo large conformational changes in the transition between "open" and "closed" states. ⁶³ We hypothesized that such residues might be

involved in siderophore binding, Tf binding, and transition-state stabilization for the iron exchange reaction. In total we pursued 8 point mutations for FhuD2 (Y256F, Y106F, R175A, W255A, Y254F, Y167F, Y169F, W173A) where Tyr residues were mutated to Phe and Arg/Trp residues were mutated to Ala (Figures 5a,d and S20; Tables S1 and S2). We evaluated the FhuD2 mutants for siderophore binding affinity (apparent $K_{\rm d}$; Table 1 and Figure S21), iron exchange with holo-Tf (Figures 5b and Figure S22), and siderophore displacement from immobilized FhuD2 (Figure 5c).

Intrinsic Trp fluorescence quenching suggested that all of the FhuD2 mutants were able to bind holo-Tf, DFOB, FOB, and FOE with nanomolar affinity resulting in apparent K_d values within the margin of error for wild-type FhuD2 (Table 1 and Figure S21). This was a surprising result, but further evaluation of the FhuD2 mutants in iron exchange and siderophore placement assays revealed some key differences in the functional relevance of this binding. Evaluation of these mutants in the siderophore displacement assay using immobilized FhuD2 mutants revealed that mutation of Tyr to Phe did not affect the efficiency of siderophore binding, while the more dramatic mutations of Arg and Trp to Ala reduced siderophore retention on the FhuD2 column. This type of binding assay more accurately reflects the concentration flux of a dynamic system and shows that W173, R175, and W255 play an important role in stabilizing the complex between FhuD2 and a siderophore ligand. Residues W173 and R175 are largely conserved among SBPs (Figure S23) and are known to form stabilizing hydrogen bonds with the hydroxamate groups of bound ferric siderophores (Figure 5a). 43,63 The loss of siderophore retention in the immobilized SBP binding study is consistent with disruption of these known stabilizing interactions. The Tyr residues form the hydrophobic cavity of the binding calyx; this property is maintained by mutation to hydrophobic Phe residues. The similar siderophore binding properties of the Tyr-to-Phe FhuD2 mutants compared to wild-type FhuD2 is consistent with a proposed role in maintaining a hydrophobic binding calyx environment. Evaluation of the FhuD2 mutants in the kinetic iron exchange assay using variable holo-Tf and saturating DFO-NBD provided valuable insight into residues involved in Tfbinding and iron shuttling steps, as reflected by apparent K_m and k_{cat} values, respectively (Table 1 and Figure 5b). The Y256F, Y106F, R175A, and W255A mutations had little effect on apparent k_{cat} but did have a general trend of increasing the apparent K_m value implying that these residues might be involved in binding holo-Tf. A clear trend emerged for three Tyr mutations (Y254F, Y167F, and Y169F) where the apparent K_m did not change relative to parent FhuD2, but the apparent $k_{\rm cat}$ was reduced, up to 4-fold, implying that these residues might be involved in the iron exchange step. It is noteworthy that the Y254F, Y167F, and Y169F were all capable of binding the siderophore cofactor similarly to wildtype FhuD2 suggesting that the Tyr hydroxyls might be directly involved in the shuttling of ferric iron possibly via transient metal coordination (Figure 5c).

The most profound effect on the apparent catalytic efficiency of FhuD2 was observed for the W173A mutant. While W173A proved critical for binding the siderophore cofactor, it appears to have no effect on the binding of *holo*-Tf. However, the W173A mutation significantly reduced the apparent $k_{\rm cat}$ by an order of magnitude (0.03 \pm 0.002) relative to wild-type FhuD2 (0.4 \pm 0.02). Therefore, the effects of the W173A mutation on

apparent k_{cat} are most likely associated with binding the siderophore cofactor, which was proven to be compromised in the siderophore displacement studies using immobilized FhuD2 (Figure 5c). Y254, Y167, Y169, and W173 are among the most dynamic residues in terms of conformational transition between the "open" and "closed" states (Figure 5d).⁶³ We hypothesized that this conformational flexibility could play a role in the metal stripping process, either by facilitating direct displacement of Tf ligands in the ferric iron coordination sphere by the siderophore hydroxamate ligands or through ligand displacement and direct metal chelation by the Tyr phenolates.

A General Ligand Exchange Mechanism Facilitates Metal Shuttling. Results from the study of FhuD2 mutants in both iron shuttling and siderophore displacement assays guided our proposal of a general working mechanism for the dual role of SBPs as ferrichelatase catalysts and permeaseassociated binding proteins in Gram-positive bacteria (Figure 6). The stoichiometry of SBP:siderophore:Tf is not entirely clear so we will assume 1:1 stoichiometry for all components according to the model proposed for vitamin B₁₂ transport via BtuCDF. 13,21-24 However, we do note there is precedent for the association of more than one SBP with a given ABC permease.⁵³ A structure of the SBP CeuE bound as a 2:2 iron:siderophore dimer has been reported.⁶⁸ There is some evidence of dimerization of FhuD2 in the solid-state crystal packing, which could support involvement of dimers in the iron shuttle. Furthermore, in P. aeruginosa there are two interacting periplasmic binding proteins, FpvC and FpvF, that associate with a single ABC permease, FpvED.⁶⁹ In this case, FpvC is homologous to metal-binding proteins and FpvF is a classic SBP which presents a scenario using two substratebinding proteins to facilitate possible metal exchange and membrane translocation.⁶⁵ Nonetheless, for FhuD2, YxeB, and related SBPs, we will assume 1:1 stoichiometries for SBP:siderophore and SBP:permease.

The resting state of surface-displayed lipid-anchored SBP is bound to a metal-free siderophore, which is present at a much higher concentration than ferric siderophores and predicted to dominate the binding equilibrium (Figure 6a). Based on functional studies of related systems, such as the vitamin B₁₂ receptor/permease BtuCDF, the "open" SBP conformation is proposed to be dissociated from the ABC permease. 13,21-24 In the case of FhuD2 and related SBPs, the N-terminal domain residue E73 and the C-terminal domain residue E206 are conserved, required for function, and proposed to facilitate favorable interactions with the permease when in the "closed" conformation (Figures 5d and S23). 63,67 In FhuD2, the Cterminal domain is more dynamic than the N-terminal domain and most of the residues implicated in the iron exchange step (Y254, Y167, Y169, and W173) are located in the C-terminal domain. 63 A nanomolar binding interaction between the SBP and holo-Tf, presumably in the "open" conformation, orients the ferric iron center for ligand exchange (Figure 6b). In holo-Tf, the ferric iron is chelated by two Tyr residues (Y95, Y188), one His residue (H249), and one Asp residue (D63) with a single molecule of carbonate filling out the octahedral coordination sphere. 54,70 There are two metal binding sites in Tf, so presumably the metal stripping takes place independently at each site. The carbonate ligand is the most labile from the iron center, so ligand exchange is proposed to be achieved via displacement of carbonate and one of the amino acid chelators (Asp displacement shown here) by the FhuD2 Tyr-triad (Y254, Y167, Y169) (Figure 6b). Interestingly, FBPs in bacteria contain a ferric iron binding site analogous to Tf where D63 is replaced by Glu suggesting that this mechanism could extend to FpvCF in *P. aeruginosa* and related organisms. 54,65,69

We propose that a flexible, metal-free siderophore cofactor might bind differently to the "open" and "closed" forms of FhuD2. Such cases of cofactor plasticity are well documented in diverse enzyme families, including the "wavin" flavin model for class A flavin-dependent monooxygenases where the flavin cofactor can adopt distinct "in" and "out" conformations.⁷¹ Notably, cofactor plasticity has been implicated in the mechanism of metal exchange catalyzed by ferrochelatases involved in the metalation of heme cofactors with ferrous iron. 57-59 In the heme ferrochelatases, protein-induced distortion of the porphoryin helps to preorganize the pyrrole ligands to lower the transition-state barrier for metal transfer. We hypothesize that a similar siderophore distortion mechanism might be at play for the siderophore-dependent ferrichelatases, FhuD2 and YxeB, during insertion of ferric iron. We showed that W173 plays an important role in siderophore cofactor binding (Figure 5c), and we propose that this residue also influences cofactor positioning. W173 is conserved among SBPs and makes a stabilizing hydrogen bonding interaction with the terminal N-acetyl hydroxamate of FOB (Figure S23).63 Crumbliss and co-workers have shown that displacement of the terminal hydroxamate ligand of linear trihydroxamate siderophores is the rate-determining step for ligand exchange on a ferric iron complex, like peeling off a bandage. W173 also makes a dramatic conformational change in the transition between "open" and "closed" forms, where a distinct "open cleft" forms in the dynamic C-terminal domain. A metalfree trihydroxamate siderophore could potentially bind in this "cryptic" site (Figure 5e,f). 63 Upon transition from "open" to "closed" form the SBP could pre-orient the siderophore cofactor to perform ligand displacement from a transient SBP-Tf mixed ferric iron complex, resulting in the formation of a ferric siderophore octahedral complex and release of apo-Tf (Figure 6c). It is also conceivable that the entire iron exchange reaction takes place from the SBP "closed" conformation with direct ligand exchange from the holo-Tf ferric iron complex by the siderophore hydroxamate ligands. After dissociation of apo-Tf, the SBP bound to ferric iron siderophore complex is free to associate with the membrane-embedded ABC permease while in the "closed" conformation (Figure 6d).

A high degree of conformational flexibility in protein scaffolds has been linked to the emergence of catalysis in non-catalytic proteins. 55,56 Protein dynamic motions have been implicated in the transfer of conformational flexibility to the bound substrate that can template evolutionary mutations in the substrate-binding pocket leading to transition-state stabilization for a given transformation resulting in the emergence of catalysis. This has been demonstrated for chalcone isomerases and cyclohexene dehydratases, which evolved from two distinct families of non-catalytic, ancestral substrate-binding proteins, namely, fatty acid binding proteins and polar amino acid binding proteins, respectively. 55,56 We have provided evidence to support that SBP calyx residues are involved in substrate binding (Y256, Y106, R175, and W255), siderophore cofactor binding (W173, R175, and W255), and metal transfer (Y254, Y167, Y169, and W173); these residues are largely conserved among SBPs (Figure S23). Two of these residues, W255 and Y254, are located on a dynamic "hinge"

region between the C-terminal and N-terminal globular domains. Y254 undergoes a 180° conformational change underneath the siderophore-binding site with the phenol pointing back toward the C-terminal helix in the "closed" conformation and in toward the siderophore-binding site in the "open" conformation where it is well-positioned to assist in the transfer of iron from holo-Tf to the bound siderophore cofactor (Figure 5d). Similar Tyr dynamics have been implicated in the shuttling of heme in *Gram*-positive bacteria. ^{32,73} W255 forms part of the hydrophobic surface of the siderophore-binding pocket in the "closed" conformation and makes a "sweeping" motion across the siderophore-binding pocket while transitioning to the "open" conformation where the indole side chain of W255 partially occupies the binding calyx region. The combined movements of Y254 and W255 might act to release the ferric iron siderophore complex from the SBP pushing it into the permease import channel to stimulate ATP hydrolysis and import to the cytoplasm (Figure 6e). While many aspects of the SBP/permease gating process are not fully appreciated, there is some structural and functional evidence for the vitamin B₁₂ BtuCDF system gathered from X-ray crystallography and single molecule fluorescence studies, respectively, that support an occluded state for the permease that opens the SBP to release the transport substrate during the translocation cycle. 13,21-24 Following siderophore translocation, the "open" SBP can dissociate from the permease to reform holo-SBP via cofactor replacement by binding a metal-free siderophore in the extracellular space (Figure 6f).

CONCLUSIONS

The underlying molecular mechanisms of metabolite translocation across bacterial membranes remain largely unexplored. Substrate-binding proteins that interface with a membraneembedded permease are often assigned a non-catalytic role as receptor in the import paradigm. Here we show that siderophore-binding proteins in Gram-positive bacteria also serve a catalytic role in a bacterial iron shuttle by acting as a siderophore-dependent ferrichelatase to strip ferric iron from holo-Tf, which is exceedingly slow at neutral pH in the absence of a catalyst. Unlike FBPs like Tf and FpvC that directly chelate ferric iron with His, Asp, Glu, and Tyr amino acid side chains, 54 here the siderophore cofactor provides the required "teeth" to chelate ferric iron. This might be a general phenomenon for surface exposed SBPs in Gram-positive bacteria as there is some evidence in S. aureus that Hts, Sir, and Sst enable the capture of iron released from human transferrin by cognate siderophores staphyloferrin A, staphyloferrin B, and catecholamine.³⁷ Catalytic SBPs might also facilitate iron shuttles in Gram-negative bacteria periplasm as acceptors of ferric iron from the "plug" domains of OMRs or periplasmic FBPs. 12,65,69 While there are dedicated pathways in many pathogenic bacteria for the removal of iron from Tf, 74,7 catalytic siderophore-dependent SBP ferrichelatases impart greater versatility for stripping metals from diverse proteins in the human metalloproteome. This new model supports growing evidence for tissue-specialized roles of siderophores and metallophores during infection to rectify the existence of seemingly redundant pathways in pathogens.⁷⁶ Insight provided by this work will help guide the exploration of SBPs as targets for the development of vaccines and siderophore-based therapeutic and diagnostic agents.

ASSOCIATED CONTENT

Supporting Information

The Supporting Information is available free of charge at https://pubs.acs.org/doi/10.1021/acscentsci.9b01257.

Experimental methods, Figures S1–S23 and Tables S1 and S2, and compound characterization data (PDF)

AUTHOR INFORMATION

Corresponding Author

Timothy A. Wencewicz — Department of Chemistry, Washington University in St. Louis, St. Louis, Missouri 63130, United States; ⊚ orcid.org/0000-0002-5839-6672; Phone: 314-935-7247; Email: wencewicz@wustl.edu; Fax: 314-935-4481

Authors

Nathaniel P. Endicott — Department of Chemistry, Washington University in St. Louis, St. Louis, Missouri 63130, United States Gerry Sann M. Rivera — Department of Chemistry, Washington University in St. Louis, St. Louis, Missouri 63130, United States Jinping Yang — Department of Chemistry, Washington University in St. Louis, St. Louis, Missouri 63130, United States

Complete contact information is available at: https://pubs.acs.org/10.1021/acscentsci.9b01257

Funding

Research was supported by start-up funds from Washington University in St. Louis, Oak Ridge Associated Universities via a Ralph E. Powe Junior Faculty Enhancement Award, NSF CAREER Award 1654611, the Alfred P. Sloan Foundation via a Sloan Fellowship, and The Camille & Henry Dreyfus Foundation via a Camille Dreyfus Teacher-Scholar Award.

Notes

The authors declare no competing financial interest.

■ ACKNOWLEDGMENTS

We thank Dr. Brad Evans at the Proteomics & Mass Spectrometry Facility at the Donald Danforth Plant Science Center, St. Louis, MO, for assistance with the acquisition of the QTRAP LC-MS/MS spectra (supported by the National Science Foundation under Grant No. DBI-0521250). We thank Prof. John-Stephen Taylor (WUSTL, Dept. of Chemistry) for assistance with fluorescence quenching studies.

ABBREVIATIONS

Dan, danoxamine; DanFe, ferric danoxamine; DanM, danoxamine macrolactone; DanMeFe, ferric danoxamine macrolactone; DFOB, desferrioxamine B; DFOE, desferrioxamine E; DFO-NBD, desferrioxamine B-2-(4-nitro-2,1,3-benzoxadiazol-7-yl) conjugate; FBP, ferric iron binding protein; FOB, ferrioxamine B; Fhu, ferric hydroxamate uptake; FOE, ferrioxamine E; FO-NBD, ferrioxamine B-2-(4-nitro-2,1,3-benzoxadiazol-7-yl) conjugate; MRSA, methicillin-resistant *Staphylococcus aureus*; OMR, outer membrane receptor; SBP, siderophore-binding protein; SDFOB, succinyldesferrioxamine B; SFOB, succinylferrioxamine B; Tf, transferrin

REFERENCES

- (1) Ratledge, C. Iron metabolism and infection. Food Nutr. Bull. 2007, 28, S515-23.
- (2) Stubbendieck, R. M.; May, D. S.; Chevrette, M. G.; Temkin, M. I.; Wendt-Pienkowski, E.; Cagnazzo, J.; Carlson, C. M.; Gern, J. E.;

- Currie, C. R. Competition among nasal bacteria suggests a role for siderophore-mediated interactions in shaping the human nasal microbiota. *Appl. Environ. Microbiol.* **2019**, *85*, No. e02406-18.
- (3) Cassat, J. E.; Skaar, E. P. Iron in infection and immunity. *Cell Host Microbe* **2013**, *13*, 509–519.
- (4) Miethke, M.; Marahiel, M. A. Siderophore-based iron acquisition and pathogen control. *Microbiol. Mol. Biol. Rev.* **2007**, *71*, 413–451.
- (5) Faraldo-Gomez, J. D.; Sansom, M. S. Acquisition of siderophores in gram-negative bacteria. *Nat. Rev. Mol. Cell Biol.* **2003**, *4*, 105–116.
- (6) Sheldon, J. R.; Heinrichs, D. E. Recent developments in understanding the iron acquisition strategies of gram positive pathogens. *FEMS Microbiol. Rev.* **2015**, *39*, 592–630.
- (7) Hider, R. C.; Kong, X. Chemistry and biology of siderophores. *Nat. Prod. Rep.* **2010**, *27*, 637–657.
- (8) Troxell, B.; Hassan, H. M. Transcriptional regulation by ferric uptake regulator (Fur) in pathogenic bacteria. *Front. Cell. Infect. Microbiol.* **2013**, 3, 59.
- (9) Moynie, L.; Milenkovic, S.; Mislin, G. L. A.; Gasser, V.; Malloci, G.; Baco, E.; McCaughan, R. P.; Page, M. G. P.; Schalk, I. J.; Ceccarelli, M.; Naismith, J. H. The complex of ferric-enterobactin with its transporter from Pseudomonas aeruginosa suggests a two-site model. *Nat. Commun.* **2019**, *10*, 3673.
- (10) Celia, H.; Noinaj, N.; Zakharov, S. D.; Bordignon, E.; Botos, I.; Santamaria, M.; Barnard, T. J.; Cramer, W. A.; Lloubes, R.; Buchanan, S. K. Structural insight into the role of the Ton complex in energy transduction. *Nature* **2016**, *538*, 60–65.
- (11) Josts, I.; Veith, K.; Tidow, H. Ternary structure of the outer membrane transporter FoxA with resolved signalling domain provides insights into TonB-mediated siderophore uptake. *eLife* **2019**, 8, No. e48528.
- (12) Stintzi, A.; Barnes, C.; Xu, J.; Raymond, K. N. Microbial iron transport via a siderophore shuttle: a membrane ion transport paradigm. *Proc. Natl. Acad. Sci. U. S. A.* **2000**, 97, 10691–10696.
- (13) Yang, M.; Livnat Levanon, N.; Acar, B.; Aykac Fas, B.; Masrati, G.; Rose, J.; Ben-Tal, N.; Haliloglu, T.; Zhao, Y.; Lewinson, O. Single-molecule probing of the conformational homogeneity of the ABC transporter BtuCD. *Nat. Chem. Biol.* **2018**, *14*, 715–722.
- (14) Stevenson, B.; Wyckoff, E. E.; Payne, S. M. Vibrio cholerae FeoA, FeoB, and FeoC interact to form a complex. *J. Bacteriol.* **2016**, *198*, 1160–1170.
- (15) Lau, C. K.; Krewulak, K. D.; Vogel, H. J. Bacterial ferrous iron transport: the Feo system. *FEMS Microbiol. Rev.* **2016**, *40*, 273–298.
- (16) Larsen, N. A.; Lin, H.; Wei, R.; Fischbach, M. A.; Walsh, C. T. Structural characterization of enterobactin hydrolase IroE. *Biochemistry* **2006**, *45*, 10184–10190.
- (17) Imperi, F.; Tiburzi, F.; Visca, P. Molecular basis of pyoverdine siderophore recycling in Pseudomonas aeruginosa. *Proc. Natl. Acad. Sci. U. S. A.* **2009**, *106*, 20440–20445.
- (18) Miethke, M.; Hou, J.; Marahiel, M. A. The siderophore-interacting protein YqjH acts as a ferric reductase in different iron assimilation pathways of Escherichia coli. *Biochemistry* **2011**, *50*, 10951–10964.
- (19) Moynie, L.; Serra, I.; Scorciapino, M. A.; Oueis, E.; Page, M. G.; Ceccarelli, M.; Naismith, J. H. Preacinetobactin not acinetobactin is essential for iron uptake by the BauA transporter of the pathogen Acinetobacter baumannii. *eLife* **2018**, *7*, No. e42270.
- (20) Bailey, D. C.; Bohac, T. J.; Shapiro, J. A.; Giblin, D. E.; Wencewicz, T. A.; Gulick, A. M. Crystal structure of the siderophore binding protein BauB bound to an unusual 2:1 complex between acinetobactin and ferric iron. *Biochemistry* **2018**, *57*, 6653–6661.
- (21) Chimento, D. P.; Mohanty, A. K.; Kadner, R. J.; Wiener, M. C. Substrate-induced transmembrane signaling in the cobalamin transporter BtuB. *Nat. Struct. Mol. Biol.* **2003**, *10*, 394–401.
- (22) Borths, E. L.; Locher, K. P.; Lee, A. T.; Rees, D. C. The structure of Escherichia coli BtuF and binding to its cognate ATP binding cassette transporter. *Proc. Natl. Acad. Sci. U. S. A.* **2002**, 99, 16642–16647.

- (23) Korkhov, V. M.; Mireku, S. A.; Locher, K. P. Structure of AMP-PNP-bound vitamin B12 transporter BtuCD-F. *Nature* **2012**, 490, 367–372.
- (24) Goudsmits, J. M. H.; Slotboom, D. J.; van Oijen, A. M. Single-molecule visualization of conformational changes and substrate transport in the vitamin B12 ABC importer BtuCD-F. *Nat. Commun.* **2017**, *8*, 1652.
- (25) Fukushima, T.; Allred, B. E.; Sia, A. K.; Nichiporuk, R.; Andersen, U. N.; Raymond, K. N. Gram-positive siderophore-shuttle with iron-exchange from Fe-siderophore to apo-siderophore by Bacillus cereus YxeB. *Proc. Natl. Acad. Sci. U. S. A.* **2013**, *110*, 13821–13826.
- (26) Fukushima, T.; Allred, B. E.; Raymond, K. N. Direct evidence of iron uptake by the Gram-positive siderophore-shuttle mechanism without iron reduction. *ACS Chem. Biol.* **2014**, *9*, 2092–2100.
- (27) Aisen, P.; Listowsky, I. Iron transport and storage proteins. *Annu. Rev. Biochem.* **1980**, 49, 357–393.
- (28) Sriyosachati, S.; Cox, C. D. Siderophore-mediated iron acquisition from transferrin by Pseudomonas aeruginosa. *Infect. Immun.* **1986**, *52*, 885–891.
- (29) Lestas, A. N. The effect of pH upon human transferrin: selective labelling of the two iron-binding sites. *Br. J. Haematol.* **1976**, 32, 341–350.
- (30) Miethke, M.; Kraushaar, T.; Marahiel, M. A. Uptake of xenosiderophores in Bacillus subtilis occurs with high affinity and enhances the folding stabilities of substrate binding proteins. *FEBS Lett.* **2013**, 587, 206–213.
- (31) Cabrera, G.; Xiong, A.; Uebel, M.; Singh, V. K.; Jayaswal, R. K. Molecular characterization of the iron-hydroxamate uptake system in Staphylococcus aureus. *Appl. Environ. Microbiol.* **2001**, *67*, 1001–1003.
- (32) Conroy, B. S.; Grigg, J. C.; Kolesnikov, M.; Morales, L. D.; Murphy, M. E. P. Staphylococcus aureus heme and siderophore-iron acquisition pathways. *BioMetals* **2019**, 32, 409–424.
- (33) Konetschny-Rapp, S.; Jung, G.; Meiwes, J.; Zahner, H. Staphyloferrin A: a structurally new siderophore from Staphylococci. *Eur. J. Biochem.* **1990**, *191*, 65–74.
- (34) Drechsel, H.; Freund, S.; Nicholson, G.; Haag, H.; Jung, O.; Zahner, H.; Jung, G. Purification and chemical characterization of staphyloferrin B, a hydrophilic siderophore from Staphylococci. *BioMetals* **1993**, *6*, 185–192.
- (35) Madsen, J. L.; Johnstone, T. C.; Nolan, E. M. Chemical synthesis of staphyloferrin B affords insight into the molecular structure, iron chelation, and biological activity of a polycarboxylate siderophore deployed by the human pathogen Staphylococcus aureus. *J. Am. Chem. Soc.* **2015**, *137*, 9117–9127.
- (36) Ghssein, G.; Brutesco, C.; Ouerdane, L.; Fojcik, C.; Izaute, A.; Wang, S.; Hajjar, C.; Lobinski, R.; Lemaire, D.; Richaud, P.; Voulhoux, R.; Espaillat, A.; Cava, F.; Pignol, D.; Borezee-Durant, E.; Arnoux, P. Biosynthesis of a broad-spectrum nicotianamine-like metallophore in Staphylococcus aureus. *Science* **2016**, 352, 1105–1109
- (37) Beasley, F. C.; Marolda, C. L.; Cheung, J.; Buac, S.; Heinrichs, D. E. Staphylococcus aureus transporters Hts, Sir, and Sst capture iron liberated from human transferrin by staphyloferrin A, staphyloferrin B, and catecholamine stress hormones, respectively, and contribute to virulence. *Infect. Immun.* **2011**, *79*, 2345–2355.
- (38) Grigg, J. C.; Cheung, J.; Heinrichs, D. E.; Murphy, M. E. P. Specificity of staphyloferrin B recognition by the SirA receptor from Staphylococcus aureus. *J. Biol. Chem.* **2010**, *285*, 34579–34588.
- (39) Grigg, J. C.; Cooper, J. D.; Cheung, J.; Heinrichs, D. E.; Murphy, M. E. P. The Staphylococcus aureus siderophore receptor HtsA undergoes localized conformational changes to enclose staphyloferrin A in an arginine-rich binding pocket. *J. Biol. Chem.* **2010**, 285, 11162–11171.
- (40) Cooper, J. D.; Hannauer, M.; Marolda, C. L.; Briere, L. A.; Heinrichs, D. E. Identification of a positively charged platform in Staphylococcus aureus HtsA that is essential for ferric staphyloferrin A transport. *Biochemistry* **2014**, *53*, 5060–5069.

- (41) Song, L.; Zhang, Y.; Chen, W.; Gu, T.; Zhang, S. Y.; Ji, Q. Mechanistic insights into staphylopine-mediated metal acquisition. *Proc. Natl. Acad. Sci. U. S. A.* **2018**, *115*, 3942–3947.
- (42) Speziali, C. D.; Dale, S. E.; Henderson, J. A.; Vines, E. D.; Heinrichs, D. E. Requirement of Staphylococcus aureus ATP-binding cassette-ATPase FhuC for iron-restricted growth and evidence that it functions with more than one iron transporter. *J. Bacteriol.* **2006**, *188*, 2048–2055.
- (43) Mariotti, P.; Malito, E.; Biancucci, M.; Lo Surdo, P.; Mishra, R. P.; Nardi-Dei, V.; Savino, S.; Nissum, M.; Spraggon, G.; Grandi, G.; Bagnoli, F.; Bottomley, M. J. Structural and functional characterization of the Staphylococcus aureus virulence factor and vaccine candidate FhuD2. *Biochem. J.* **2013**, *449*, 683–693.
- (44) Sebulsky, M. T.; Heinrichs, D. E. Identification and characterization of fhuD1 and fhuD2 two genes involved in iron-hydroxamate uptake in Staphylococcus aureus. *J. Bacteriol.* **2001**, *183*, 4994–5000.
- (45) Sebulsky, M. T.; Speziali, C. D.; Shilton, B. H.; Edgell, D. R.; Heinrichs, D. E. FhuD1, a ferric hydroxamate-binding lipoprotein in Staphylococcus aureus: a case of gene duplication and lateral transfer. *J. Biol. Chem.* **2004**, 279, 53152–53159.
- (46) Gwinner, T. Das Siderophore-Antibiotikum Salmycin. Ph.D. Thesis, Eberhard Karls Universitat Tubingen, Tubingen, Germany, 2008
- (47) Braun, V.; Pramanik, A.; Gwinner, T.; Koberle, M.; Bohn, E. Sideromycins: tools and antibiotics. *BioMetals* **2009**, *22*, 3–13.
- (48) Zheng, T.; Nolan, E. M. Siderophore-based detection of Fe(III) and microbial pathogens. *Metallomics* **2012**, *4*, 866–880.
- (49) Au-Yeung, H. Y.; Chan, J.; Chantarojsiri, T.; Chang, C. J. Molecular imaging of labile iron(II) pools in living cells with a turn-on fluorescent probe. *J. Am. Chem. Soc.* **2013**, *135*, 15165–15173.
- (50) Bar-Ness, E.; Hadar, Y.; Chen, Y.; Shanzer, A.; Libman, J. Iron uptake by plants from microbial siderophores: a study with 7-nitrobenz-2 oxa-1,3-diazole-desferrioxamine as fluorescent ferrioxamine B analog. *Plant Physiol.* **1992**, *99*, 1329–1335.
- (51) Endicott, N. P.; Lee, E.; Wencewicz, T. A. Structural basis for xenosiderophore utilization by the human pathogen Staphylococcus aureus. *ACS Infect. Dis.* **2017**, *3*, 542–553.
- (52) Rivera, G. S. M.; Beamish, C. R.; Wencewicz, T. A. Immobilized FhuD2 siderophore-binding protein enables purification of salmycin sideromycins from Streptomyces violaceus DSM 8286. *ACS Infect. Dis.* **2018**, *4*, 845–859.
- (53) Berntsson, R. P.; Smits, S. H.; Schmitt, L.; Slotboom, D. J.; Poolman, B. A structural classification of substrate-binding proteins. *FEBS Lett.* **2010**, *584*, 2606–2617.
- (54) Krewulak, K. D.; Vogel, H. J. Structural biology of bacterial iron uptake. *Biochim. Biophys. Acta, Biomembr.* **2008**, *1778*, *1781*–1804.
- (55) Kaltenbach, M.; Burke, J. R.; Dindo, M.; Pabis, A.; Munsberg, F. S.; Rabin, A.; Kamerlin, S. C. L.; Noel, J. P.; Tawfik, D. S. Evolution of chalcone isomerase from a noncatalytic ancestor. *Nat. Chem. Biol.* **2018**, *14*, 548–555.
- (56) Clifton, B. E.; Kaczmarski, J. A.; Carr, P. D.; Gerth, M. L.; Tokuriki, N.; Jackson, C. J. Evolution of cyclohexadienyl dehydratase from an ancestral solute-binding protein. *Nat. Chem. Biol.* **2018**, *14*, 542–547.
- (57) Wu, C. K.; Dailey, H. A.; Rose, J. P.; Burden, A.; Sellers, V. M.; Wang, B. C. The 2.0 A structure of human ferrochelatase, the terminal enzyme of heme biosynthesis. *Nat. Struct. Biol.* **2001**, *8*, 156–160.
- (58) Karlberg, T.; Hansson, M. D.; Yengo, R. K.; Johansson, R.; Thorvaldsen, H. O.; Ferreira, G. C.; Hansson, M.; Al-Karadaghi, S. Porphyrin binding and distortion and substrate specificity in the ferrochelatase reaction: the role of active site residues. *J. Mol. Biol.* **2008**, *378*, 1074–1083.
- (59) Al-Karadaghi, S.; Franco, R.; Hansson, M.; Shelnutt, J. A.; Isaya, G.; Ferreira, G. C. Chelatases: distort to select? *Trends Biochem. Sci.* **2006**, *31*, 135–142.
- (60) Ghosh, A.; Smith, P. E. S.; Qin, S.; Yi, M.; Zhou, H. X. Both Ligands and macromolecular crowders preferentially bind to closed

- conformations of maltose binding protein. *Biochemistry* **2019**, 58, 2208–2217.
- (61) D'Onofrio, A.; Crawford, J. M.; Stewart, E. J.; Witt, K.; Gavrish, E.; Epstein, S.; Clardy, J.; Lewis, K. Siderophores from neighboring organisms promote the growth of uncultured bacteria. *Chem. Biol.* **2010**, *17*, 254–264.
- (62) Chu, B. C. H.; Otten, R.; Krewulak, K. D.; Mulder, F. A. A.; Vogel, H. J. The solution structure, binding properties, and dynamics of the bacterial siderophore-binding protein FepB. *J. Biol. Chem.* **2014**, 289, 29219–29234.
- (63) Podkowa, K. J.; Briere, L. A.; Heinrichs, D. E.; Shilton, B. H. Crystal and solution structure analysis of FhuD2 from Staphylococcus aureus in multiple unliganded conformations and bound to ferrioxamine-B. *Biochemistry* **2014**, *53*, 2017–2031.
- (64) Amaral, M.; Kokh, D. B.; Bomke, J.; Wegener, A.; Buchstaller, H. P.; Eggenweiler, H. M.; Matias, P.; Sirrenberg, C.; Wade, R. C.; Frech, M. Protein conformational flexibility modulates kinetics and thermodynamics of drug binding. *Nat. Commun.* **2017**, *8*, 2276.
- (65) Banerjee, S.; Weerasinghe, A. J.; Parker Siburt, C. J.; Kreulen, R. T.; Armstrong, S. K.; Brickman, T. J.; Lambert, L. A.; Crumbliss, A. L. Bordetella pertussis FbpA binds both unchelated iron and iron siderophore complexes. *Biochemistry* **2014**, *53*, 3952–3960.
- (66) Raines, D. J.; Moroz, O. V.; Blagova, E. V.; Turkenburg, J. P.; Wilson, K. S.; Duhme-Klair, A. K. Bacteria in an intense competition for iron: Key component of the Campylobacter jejuni iron uptake system scavenges enterobactin hydrolysis product. *Proc. Natl. Acad. Sci. U. S. A.* 2016, 113, 5850–5855.
- (67) Sebulsky, M. T.; Shilton, B. H.; Speziali, C. D.; Heinrichs, D. E. The role of FhuD2 in iron(III)-hydroxamate transport in Staphylococcus aureus. Demonstration that FhuD2 binds iron(III)-hydroxamates but with minimal conformational change and implication of mutations on transport. *J. Biol. Chem.* **2003**, 278, 49890–49900.
- (68) Raines, D. J.; Moroz, O. V.; Wilson, K. S.; Duhme-Klair, A. K. Interactions of a periplasmic binding protein with a tetradentate siderophore mimic. *Angew. Chem., Int. Ed.* **2013**, *52*, 4595–4598.
- (69) Brillet, K.; Ruffenach, F.; Adams, H.; Journet, L.; Gasser, V.; Hoegy, F.; Guillon, L.; Hannauer, M.; Page, A.; Schalk, I. J. An ABC transporter with two periplasmic binding proteins involved in iron acquisition in Pseudomonas aeruginosa. ACS Chem. Biol. 2012, 7, 2036–2045.
- (70) MacGillivray, R. T. A.; Moore, S. A.; Chen, J.; Anderson, B. F.; Baker, H.; Luo, Y.; Bewley, M.; Smith, C. A.; Murphy, M. E. P.; Wang, Y.; Mason, A. B.; Woodworth, R. C.; Brayer, G. D.; Baker, E. N. Two high-resolution crystal structures of the recombinant N-lobe of human transferrin reveal a structural change implicated in iron release. *Biochemistry* 1998, 37, 7919–7928.
- (71) Park, J.; Gasparrini, A. J.; Reck, M. R.; Symister, C. T.; Elliott, J. L.; Vogel, J. P.; Wencewicz, T. A.; Dantas, G.; Tolia, N. H. Plasticity, dynamics, and inhibition of emerging tetracycline resistance enzymes. *Nat. Chem. Biol.* **2017**, *13*, 730–736.
- (72) Monzyk, B.; Crumbliss, A. L. Kinetics and mechanism of the stepwise dissociation of iron(III) from ferrioxamine B in aqueous acid. *J. Am. Chem. Soc.* **1982**, *104*, 4921–4929.
- (73) Bowden, C. F. M.; Chan, A. C. K.; Li, E. J. W.; Arrieta, A. L.; Eltis, L. D.; Murphy, M. E. P. Structure-function analyses reveal key features in Staphylococcus aureus IsdB-associated unfolding of the heme-binding pocket of human hemoglobin. *J. Biol. Chem.* **2018**, 293, 177–190.
- (74) Modun, B.; Williams, P. The staphylococcal transferrin-binding protein is a cell wall glyceraldehyde-3-phosphate dehydrogenase. *Infect. Immun.* **1999**, *67*, 1086–1092.
- (75) Noinaj, N.; Buchanan, S. K.; Cornelissen, C. N. The transferriniron import system from pathogenic Neisseria species. *Mol. Microbiol.* **2012**, *86*, 246–257.
- (76) Perry, W. J.; Spraggins, J. M.; Sheldon, J. R.; Grunenwald, C. M.; Heinrichs, D. E.; Cassat, J. E.; Skaar, E. P.; Caprioli, R. M. Staphylococcus aureus exhibits heterogeneous siderophore produc-

tion within the vertebrate host. *Proc. Natl. Acad. Sci. U. S. A.* **2019**, 116, 21980–21982.